Journal of Materials and Environmental Sciences
ISSN : 2028-2508

JMES, 2017 Volume 8, Issue 4, Page 1391-1400

http://www.jmaterenvironsci.com /

Quantum calculations to construct a 3D-QSAR model based on PCP-TCP derivatives and Molecular Docking with NMDA receptor

Charif EL M'BARKI, Menana ELHALLAOUI

Engineering Materials, Modeling and Environmental Laboratory, group of computational chemistry. Department of chemistry, Faculty of Science, University Sidi Mohammed Ben Abdellah, B.P. 1796, Atlas, Fes, Morocco.

Received 10 Aug 2016,
Revised 07 Feb2017,
Accepted 12 Feb 2017

Keywords

- ✓ Inhibition activity,
- ✓ 3D-QSAR model,
- ✓ MLR,
- ✓ ANN,
- ✓ LOO,
- ✓ Docking

charif.elmbarki@usmba.ac.ma

Abstract

In order to investigate the relationship between $K_{0.5}$ activities and structures of PCP and TCP derivatives, QSAR studies are applied on a series of 37 compounds by using the multiple linear regression method (MLR), and artificial neural network (ANN) techniques considering the relevant descriptors obtained from the MLR. Density functional theory (DFT) and ab-initio molecular orbital calculations have been carried out in order to get insights into the structure, so, main informations of the general properties are provided. So, As a result of quantitative structure-activity relationship of PCP and TCP derivatives, we found that the model proposed in this study is constituted of major descriptors used to describe these molecules as dipole moment and total energy. A correlation coefficient of 0.9436 was obtained with 4-3-1 ANN model. This model is statistically significant and shows very good stability towards data variation in leave-one-out (LOO) cross-validation (R_{cv} =0.9149). The docking of PCP and some derivatives show that the nitrogen hydrogen bonding is essential to enhance activity at NMDA receptor. In the other hand the docking of compounds 19, 20 and 21 reveals the impact of steric effect in decreasing activity.

1. Introduction

Phencyclidine (PCP) is a psychomimetic drug that was originally developed as a general (Sernyl®). PCP induces schizophrenia-like symptoms in healthy humans and exacerbates existing symptoms in stabilized patients with schizophrenia **[1]**. Common symptoms of schizophrenia are usually classified into two categories, positive and negative symptoms **[2-8]**. A typical psychostimulant such as methamphetamine generally induces only positive symptoms and induces few negative symptoms, or can even improve negative symptoms **[9-10]**. In contrast, PCP-induced psychosis involves both positive and negative symptoms, as well as cognitive dysfunction (disturbed attention and working memory) **[11-14]**. In non-human animals, systemic administration of PCP also produces cognitive and behavioral abnormalities that correspond to the symptoms of schizophrenia **[15]**. Furthermore, PCP-treated animals exhibited poor performance in a delayed-response task **[16]**, indicating disturbance in working memory; a typical cognitive deficit in patients with schizophrenia. PCP-treated animals provide a useful pharmacological model of schizophrenia, and there is a great interest in understanding the neural mechanisms by which PCP modulates behavior. However, the neural mechanisms involved in the development of PCP-induced psychosis remain unclear. Therefore, the development of new alternative psychomimetic drugs devoid of side effects is still needed. Therefore, to find the structural requirements for more active psychotomimetic agents, comparative QSAR studies remains the alternative mean in this area. The quantitative structure-activity relationships (QSAR) are certainly a major factor in contemporary drug design. Thus, it's quite clear why a large number of users of QSAR **[17, 18]** are located in industrial research units. So, classical QSAR and 3D-QSAR are highly active areas of research in drug design **[19, 20]**. In attempt to set up a 3D-QSAR model able to predict inhibitory activity of new molecules, we applied in this work appropriate QSAR tools, Multiple Linear Regression (MLR) analysis and Artificial Neural Network (ANN), to a series of 37 derivatives of N-(1-phenylcyclohexyl)piperidine. In a final section, molecular docking of PCP and derivatives is carried out in an attempt to understand the mode of interaction between ligands and receptor site.

2. Materials and Methods

2.1. Experimental data

The 3D-QSAR studies were performed on 37 arylcyclohexylamines including PCP and TCP derivatives (Table 1) that is reported by Chaudieu et al **[21]**. The inhibitory activities of the compounds cover a wide range of

biological activity spanning over five log units (0.017-370 µM) and diverse structural features. In this work, The $K_{0.5}$ values were converted into $logK_{0.5}$ for use in the QSAR studies.

Table 1: Structures and activities of the arylcyclohexylamines derivatives

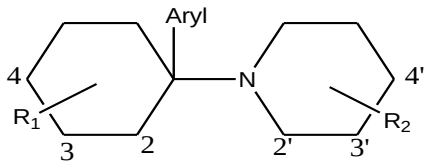

No	Aryl*	R_1+	R_2	$logK_{0.5}$	$K_{0.5}$
1	Ph	H	H	-0.6021	0.250
2	Ph	4-tButyl-cis	H	2.0000	100.000
3	Ph	4-tButyl-trans	H	2.0170	104.000
4	Ph	4-Methyl-cis	H	-0.3010	0.500
5	Ph	4-Methyl-trans	H	-0.8861	0.130
6	Ph	3-Methyl-cis	H	-0.2218	0.600
7	Ph	4- Methyl-trans	H	-0.2218	0.600
8	Ph	2- Methyl-cis	H	-0.9208	0.120
9	Ph	2- Methyl-trans	H	0.2041	1.600
10	Ph	2-Methoxy-trans	H	0.6989	0.500
11	Ph	2-Methoxy-cis	H	-0.0809	0.830
12	Ph	4,4-diMethyl	H	0.6989	5.000
13	Ph	$2\text{-}(CH_2)_3\text{-}6$	H	0.6721	4.700
14	Ph	3,3-diMethyl 5-Methyl-cis	H	0.7993	6.300
15	Ph	3,3-diMethyl 5-Methyl-cis	H	1.0000	10.000
16	Ph	H	4'-Hydroxyl	0.3424	2.200
17	Ph	H	3'Methyl	-0.7959	0.160
18	m-Nitro-Ph	H	H	1.0607	11.500
19	p-Hydroxy-Ph	H	H	1.3010	20.000
20	m-Hydroxy-Ph	H	H	-1.5229	0.030
21	o-Hydroxy-Ph	H	H	-0.1249	0.750
22	m-Methoxy-Ph	H	H	-1.0458	0.090
23	p,m-diMethoxy-Ph	H	H	0.9777	9.500
24	p-Methoxy-Ph	4-Methyl-cis	H	0.6812	4.800
25	p-Methoxy-Ph	4-Methyl-trans	H	0.3424	2.200
26	m-Methoxy-Ph	4-Methyl-cis	H	-1.3565	0.440
27	m-Methoxy-Ph	4-Methyl-trans	H	-1.2366	0.058
28	2-Th	H	H	-1.5850	0.026
29	2-Th	2-Methyl-cis	H	-1.3979	0.040
30	2-Th	2-Methyl-trans	H	0.0000	1.000
31	2-Th	4-tButyl-trans	H	2.0000	100.000
32	2-Th	4-tButyl-cis	H	2.5682	370.000
33	2-Th	4-Methyl-cis	H	0.0000	1.000
34	2-Th	4-Methyl-trans	H	-0.8539	0.140
35	2-Th	4-Hydroxy-trans	H	0.9031	8.000
36	2-Th	H	3',4' desH	-1.7696	0.017
37	2-BzTh	H	H	0.8325	6.800

*Ph = Phenyl, Th = Thienyl, BzTh = Benzothiophenyl, desH = dehydrogenation

+Cis/trans refers to the relative positions of piperidine and the substituent R_1.

$K_{0.5}$ is concentration of unlabeled derivatives which prevent 50% of the maximal specific binding determined in the absence of unlabeled derivative.

2.2. Calculation of molecular descriptors

For each compound, the electronic descriptors were obtained from quantum chemical calculations. These global electronic descriptors that are defined on the basis of density functional theory have been widely used in SAR/QSAR investigations **[22, 23]**. All the compounds were fully optimized with the density functional theory (DFT)/B3LYP level of theory **[24, 25]**, combined with the 6-31G basis set. All the calculations were performed by using the Gaussian 03 package of programs **[26]**. The rest of representative descriptors were calculated with Chem3D Ultra (version 8.0) and ACD/ChemSketch program **[27]**.

Table 2: Descriptors chosen for the QSAR model, and used in this study

Category of descriptors	Description	Notation
Electronic	Dipole moment	Dp
	Electronegativity	X
	Total energy	E
	Electron affinity	A
	Hardness	H
	Softness	S
	Polarisability	P
	Dipole Length	DL
	Reactivity	R
	Reactivity index	Ω
thermodynamic	Molar refractivity	MR
	Log P	logP
	Critical Temperature	Tc
	Melting Point	MP
steric	Sum Of Valence Degrees	SVDe
	Cluster Count	ClsC
Physicochemical	Parachor	Pc
Optic	Refraction index	n

2.3. Statistical analysis

2.3.1. Multiple linear regressions

The statistic technique multiple linear regression is used to study the relation between one dependent variable and several independent variables. It is a mathematic technique that minimizes differences between actual and predicted values. The multiple linear regression model (MLR) was generated using the software SYSTAT, version 13, to predict inhibitory activity $\log K_{0.5}$. It has served also to select the descriptors used as the input parameters for a back propagation network (ANN). In this work four descriptors have been selected, details of calculations are given in the results paragraph.

2.3.2. Artificial neural networks (ANNs)

All the feed-forward ANN used in this paper are three-layer networks; the input layer contains four neurons, representing the relevant descriptors obtained in MLR technique. Although there are neither theoretical nor empirical rules to determine the number of hidden layers or the number of neurons layers, one hidden layer seems to be sufficient in the most chemical application of ANN. Some authors **[28, 29]** have proposed a parameter ρ, leading to determine the number of hidden neurons, which plays a major role in determining the best ANN architecture. It's defined as follows:

$$\rho = \frac{Number\ of\ data\ points\ in\ the\ training\ set}{Sum\ of\ the\ number\ of\ connections\ in\ the\ NN}$$

Therefore, in order to avoid overfitting or underfitting, it's recommended to take into account the ρ value; $1.8 < \rho < 2.3$ **[30]**. Thus, the ANN used in this work is formed by three hidden neurons, and the output layer represents the calculated activity values $\log K_{0.5}$.

So, the final ANN architecture is [4-3-1], it's depicted in figure 1.

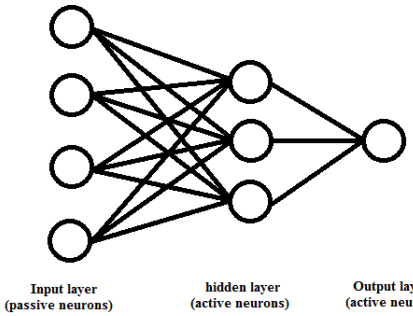

Figure 1: Schematic representation of the three-layer neural network architecture [4-3-1]

2.3.3. Cross-validation technique

Cross-validation is a popular technique used to explore the reliability of statistical models. Based on this technique, a number of modified data sets are created by deleting in each case one or a small group of molecules, these procedures are named respectively "leave-one-out" and "leave-some-out" **[31, 32]**. For each data set, an input-output model is developed. The model is evaluated by measuring its accuracy in predicting the responses of the remaining data (those that were not used in the development of the model). In this study we used, the leave-one-out (LOO) procedure.

Table 3 summarized handpicked descriptors values, observed activities, and MLR, ANN and CV predicted activities.

Table 3: Values of the selected descriptors, and the observed/predicted $logK_{0.5}$ values

Coumpound	Log(-E)	ClsC	SVDe	Dp	$LogK_{0.5}$(obs)	$LogK_{0.5}$(calc)		
						MLR	ANN	LOO
1	6.5757	18	48	0.3496	-0.6021	-1.0165	-0.6019	-0.8289
2	6.7738	22	56	0.3802	2.0000	1.7752	1.9954	2.0251
3	6.7738	22	56	0.3478	2.0170	1.7369	1.9804	1.8432
4	6.6290	19	50	0.3244	-0.3010	-0.3714	-0.5497	-0.4468
5	6.6290	19	50	0.3657	-0.8861	-0.3227	-0.5043	-0.3656
6	6.6290	19	50	0.4092	-0.2218	-0.2713	-0.4569	-0.2407
7	6.6290	19	50	0.2950	-0.2218	-0.4061	-0.5817	-0.6329
8	6.6290	19	50	0.3178	-0.9208	-0.3792	-0.5573	-.4371
9	6.6290	19	50	0.4110	0.2041	-0.2692	-0.4549	-0.1829
1	6.7237	20	56	1.5853	0.6989	-0.1668	0.6977	-0.0670
11	6.7237	20	56	1.4802	-0.0809	-0.2909	-0.2477	-0.0360
12	6.6797	20	52	0.3680	0.6989	0.3648	0.5670	0.7521
13	6.7264	21	56	0.8749	0.6721	0.7598	0.8455	0.6655
14	6.7278	21	54	0.3824	0.7993	1.0757	1.3872	1.0798
15	6.7278	21	54	0.2818	1.0000	0.9569	1.3241	0.9516
16	6.6753	19	54	2.3809	0.3424	0.0795	0.3400	0.3258
17	6.6290	19	50	0.3063	-0.7959	-0.3928	-0.5695	-0.6495
18	6.8264	21	66	5.3161	1.0607	1.1191	1.1132	1.1036
19	6.6753	19	54	1.7960	1.3010	-0.6112	0.4877	-0.4680
20	6.6754	19	54	1.7792	-1.5229	-0.6311	-1.3393	-0.0770
21	6.6753	19	54	1.8138	-0.1249	-0.5902	0.5254	-0.1243
22	6.7237	20	56	1.9006	-1.0458	0.2055	-0.5853	-0.0061
23	6.8527	22	64	2.8600	0.9777	0.7997	0.9775	1.0129
24	6.7699	21	58	1.6832	0.6812	0.6501	0.3241	0.9672
25	6.7699	21	58	1.6782	0.3424	0.6442	0.3197	0.2855
26	6.7699	21	58	1.2094	-0.3565	0.0906	-0.3391	-0.6796
27	6.7699	21	58	1.2336	-1.2366	0.1192	-1.2608	-0.4895
28	6.9452	17	42.6667	0.8359	-1.5850	-1.1797	-1.9076	-1.6796
29	6.9824	18	44.6667	0.7998	-1.3979	-0.4875	-0.4859	-0.6138
30	6.9824	18	44.6667	1.0140	0.0000	-0.2346	-0.2583	-0.1362
31	7.0862	21	50.6667	0.8631	2.0000	1.8198	2.0908	2.4819
32	7.0862	21	50.6667	0.8463	2.5682	1.7999	2.0834	2.1433
33	6.9824	18	44.6667	0.8261	0.0000	-0.4565	-0.4573	-0.6461
34	6.9824	18	44.6667	0.8513	-0.8538	-0.4268	-0.4301	-0.6880
35	7.0151	18	44.6667	2.4088	0.9031	1.2909	0.8729	0.9582
36	6.9440	17	44.6667	0.6806	-1.7696	-2.2616	-1.6785	-1.6407
37	7.0831	21	56.6667	2.1603	0.8325	0.6546	0.5105	0.8451

2.3.4. Docking method

Molecular docking is performed with Hex8.0.0 software **[33]**. The native structure of NMDA receptor (figure 2) was retrieved from Brookhaven protein data bank (2HQW.PDB) **[34]**. Ligands are built and optimized with chem3D Ultra 8.0 software and the docked conformations were viewed using PyMOL software package **[35]**. PCP molecule is explored with two configurations, axial and equatorial positions of phenyl ring (figure 3), and default parameters are used for docking process used for docking process.

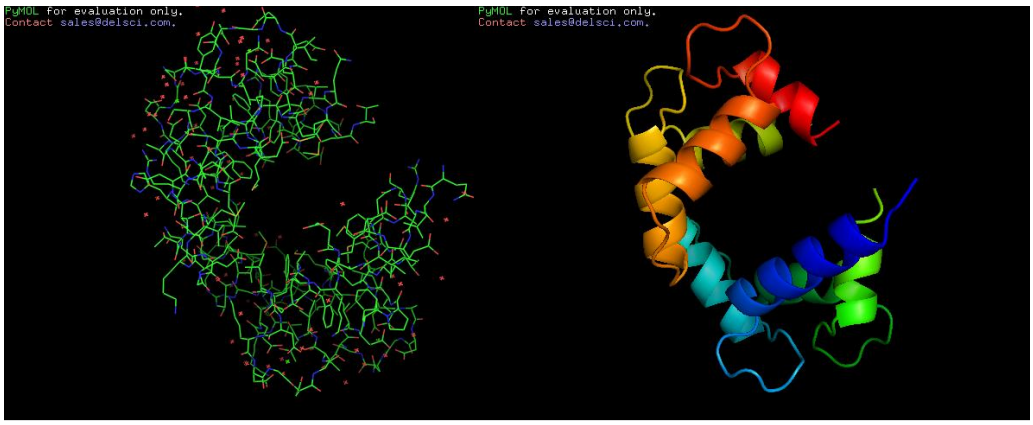

Figure 2: Structure of N-methyl-D-aspartate receptor (NMDA)

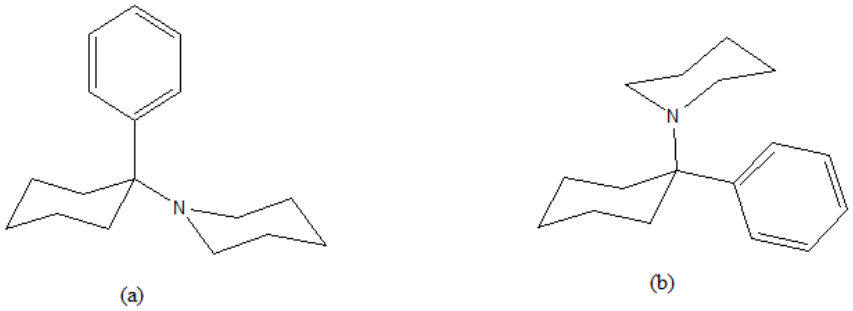

Figure 3: Structure of PCP with phenyl in axial (a) and equatorial (b) position

3. Results and discussion

3.1. Multiple Linear Regressions

Many attempts have been made to develop a relationship with the indicator variable of inhibitory activity $\log K_{0.5}$, but the best relationship obtained by this method is only one corresponding to the linear combination of several descriptors: the total energy (-logE), the dipole moment (Dp), cluster count (ClsC) and sum of valence degrees (SVDe). The QSAR model built using multiple linear regression (MLR) method is represented by the following equation:

$$\mathbf{\log K_{0.5}} = 12.656 - 3.707\ \mathbf{(-logE)} + 1.775\ \mathbf{(ClsC)} - 0.451\ \mathbf{(SVDe)} + 1.181\ \mathbf{(Dp)}$$

$$N = 37 \qquad R = 0.832 \qquad R^2 = 0.693 \qquad RMSE = 0.644 \qquad F\text{-ratio} = 18.055$$

Where N is the number of compounds, R is the correlation coefficient, RMSE is the standard error of estimate and F is the Fisher F-statistic.

For the 37 compounds series, the correlation between observed inhibitory activities and calculated ones based on this model are quite significant as indicated by statistical values.

The correlation of the observed activities with the MLR calculated ones is illustrated in figure 4. Figure 4 shows a very regular distribution of inhibitory activities values depending on the observed values.

3.2. Artificial neural networks (ANNs)

In order to increase the probability of good characterization of studied compounds, neural networks (ANN) used to generate predictive models of quantitative-activity relationships (QSAR) between the set of MLR selected molecular descriptors and observed activities. The correlation between observed inhibitory activities and ANN calculated values are illustrated in figure 5.

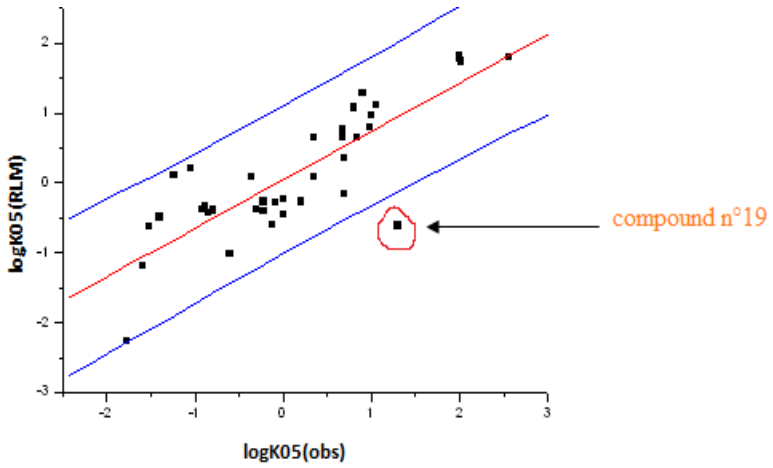

Figure 4: Plot of observed versus (MLR) predicted inhibitory activities

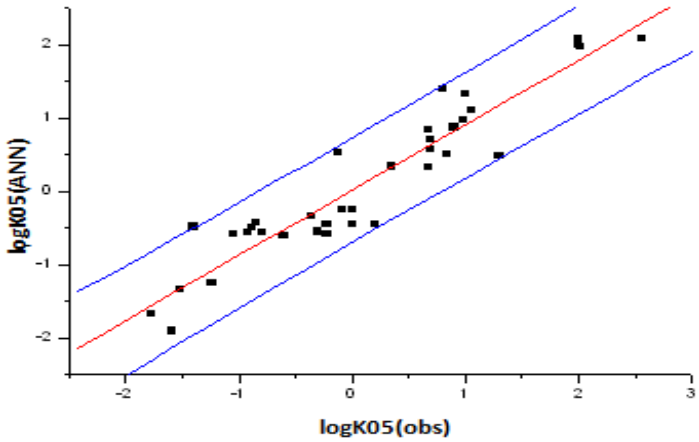

Figure 5: Plot of observed versus (ANN) predicted inhibitory activities

N = 37 R = 0.9436 R^2 = 0.8904 RMSE = 0.8133

The correlation coefficient and standard error of estimate obtained with the neural network, show that the selected descriptors by MLR are pertinent and that the model proposed to predict activity is relevant.

3.3. Cross validation (CV)

Before using a QSAR model to predict the activity of new compounds, we should validate it using a validation method. In this paper we validate our model (NN model) obtained with neural network method, with cross validation using LOO procedure. The correlation of the observed activities with the CV calculated ones is illustrated in figure 6.

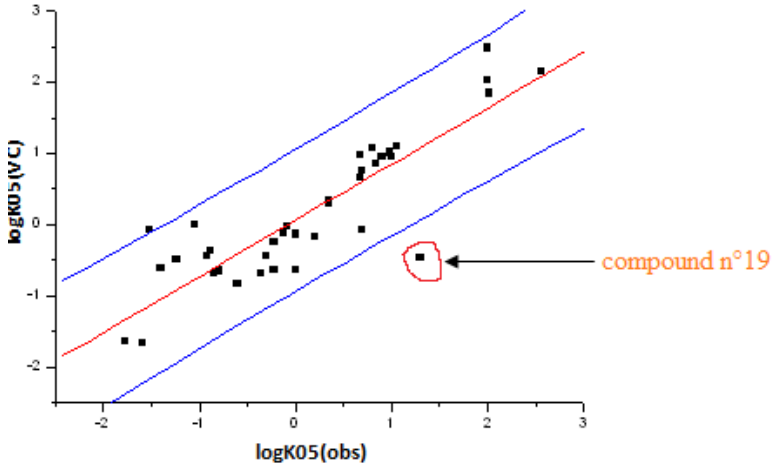

Figure 6: Plot of observed versus CV predicted inhibitory activities

N = 37 R = 0.8751 R^2 = 0.7659

Compound 19 is considered as an outlier point in this series, in fact the elimination of this compound in the calculation of the correlation coefficient shows a significant improvement in the correlation. The correlation of the observed activities with the CV calculated ones without atypical point is illustrated in figure 7.

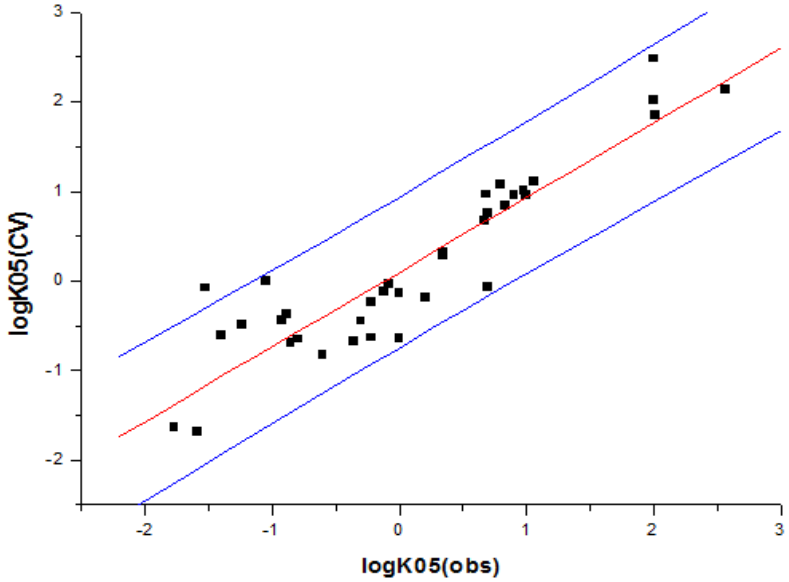

Figure 7: Plot of observed versus (**CV**) predicted inhibitory activities without atypical point
N = 36 R = 0.9149 R^2 = 0.837

The good correlation obtained in cross-validating the model with the full set R_{cv} = 0.8751 and that without atypical point R_{cv} = 0.9149 show that the predictive power of this model is very significant. So, the most important result of this investigation is that in vitro inhibitory activities could be predicted using QSAR model. In fact, the model proposed in this study shows high predictive power. One of the most important observations that can be drawn from this study is that different descriptors representing the majority of descriptors proposed to build a QSAR model were selected.

3.4. Docking

The fact that the non active compound 19, having a hydroxyl group in para position, is considered as an outlier point in MLR and CV investigations, prompted us to the docking of this molecule with the NMDA receptor in the order to understand how it interacts with the binding site. We proceed the same with compound 20 and 21 having an hydroxyl in meta and ortho positions, respectively. The docking of compounds 19, 20 and 21 with NMDA receptor is illustrated in figures 8, 9 and 10. Schemas in the right of the figures illustrate the zoom of the interaction between the ligand and the binding site.

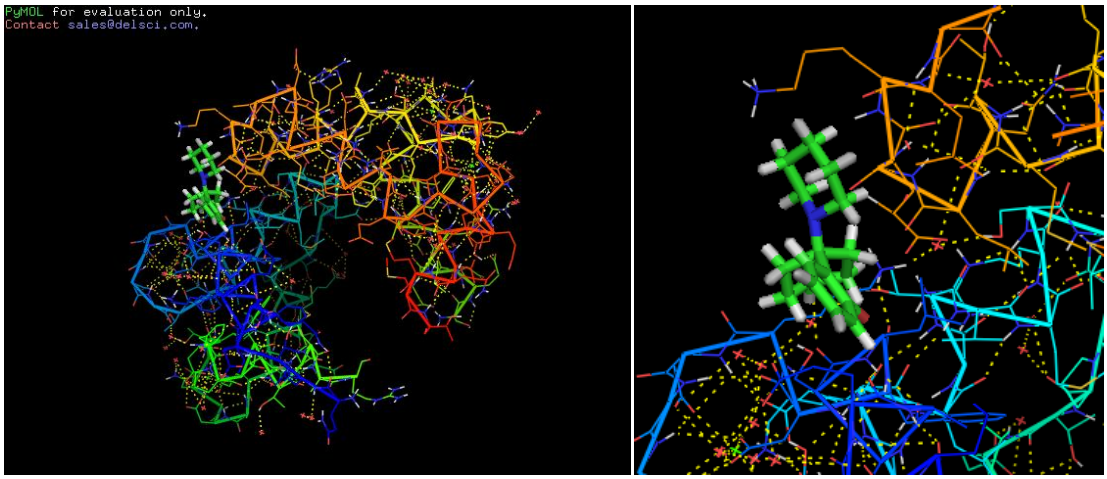

Figure 8: Docking of compound 19 with NMDA receptor

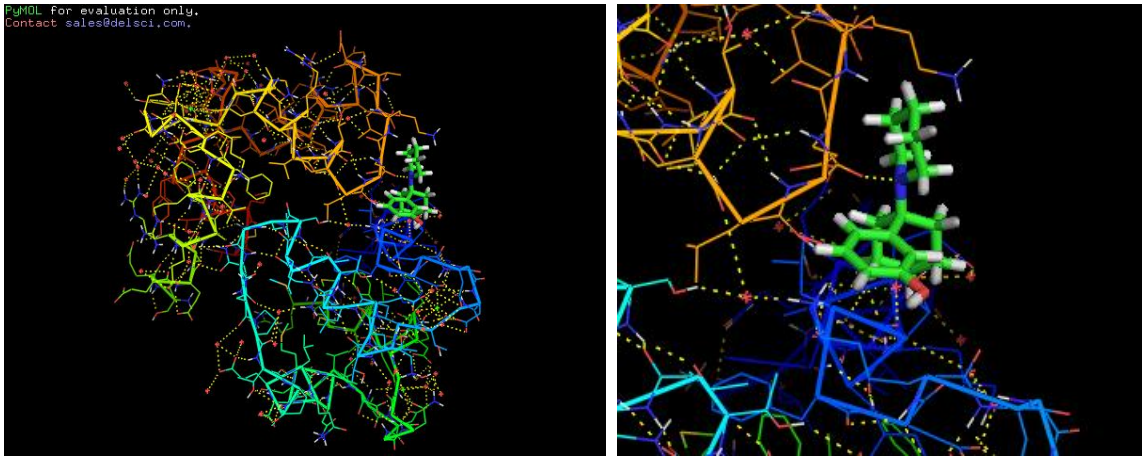

Figure 9: Docking of compound 20 with NMDA receptor

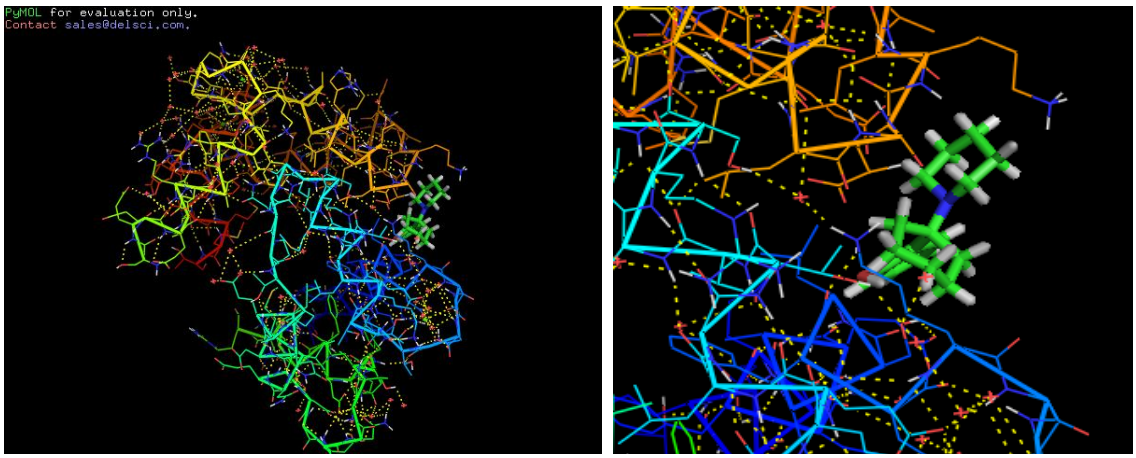

Figure 10: Docking of compound 21 with NMDA receptor

We observe that Compounds 19 and 21 don't form hydrogen bonding through N atom when docked to NMDA protein; moreover these compounds could not penetrate into the binding site, which could be explained by the steric effect caused by ortho and para-substituants. However compound 20 shows hydrogen bonding between nitrogen and hydroxyl group which explain the potential activity of this compound. The docking of PCP, with phenyl in axial and equatorial positions, with NMDA receptor is illustrated respectively in figures 11 and 12.

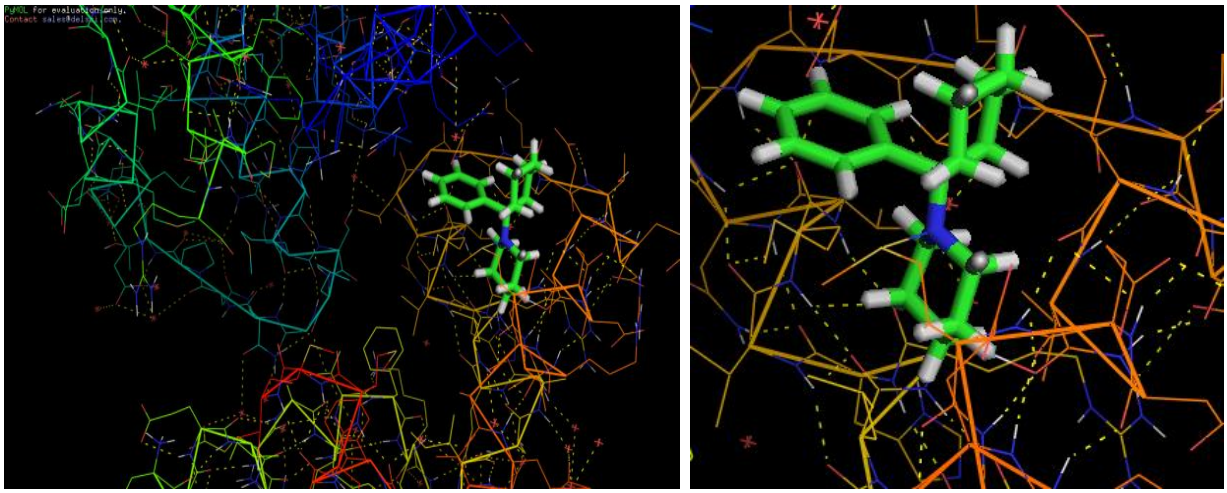

Figure 11: Docking of PCP with phenyl in axial position

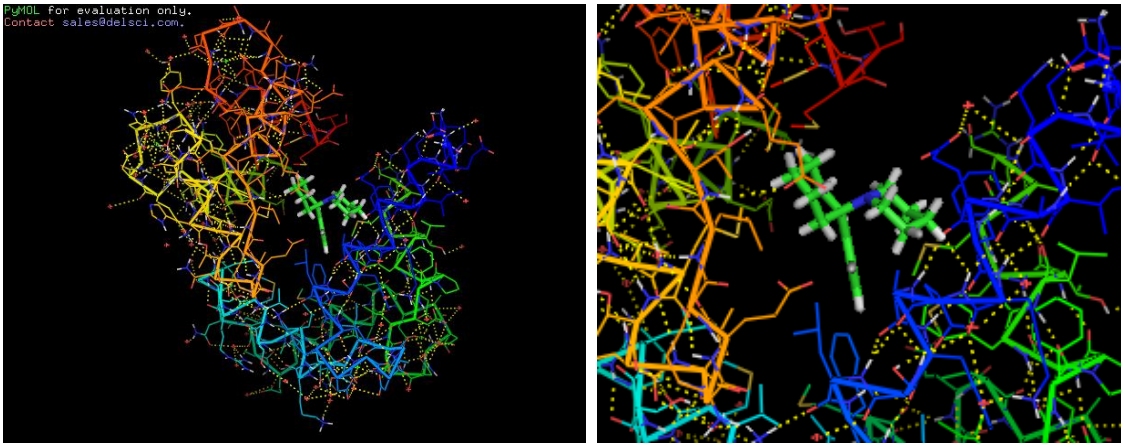

Figure 12: Docking of PCP with phenyl in equatorial position

Schemas in the right of the figures illustrate the zoom of the interaction between the ligand and the binding site. The docking of PCP with the NMDA receptor reveals that the appropriate conformation of PCP is that with phenyl in position axial, in fact with this conformation the nitrogen is able to make hydrogen bonding with sulfur atom (figure 11) however with the equatorial position we don't observe this hydrogen bonding (Figure 12).

Conclusion

In this work, we have explored a set of 37 compounds of PCP and TCP derivatives using QSAR tools. The analysis methods, multiple linear regression (RLM), neural network (NN) and cross validation using LOO procedure (CV) applied to the series of PCP and TCP derivatives, allowed us to select the relevant descriptors that could have influence on the activity. The analysis of the Inhibitory activities model suggests that the descriptors representing high interest for activity are total energy, dipole moment, cluster count and sum of valence degrees. Artificial neural network (ANN) techniques, considering the relevant descriptors obtained from the MLR, showed good agreement between the observed and the predicted values. To test the performance of this model, we have used leave-one-out method (R_{cv}=0.9149) which showed that the model proposed in this work is able to accurately predict the activity. Molecular docking of PCP and derivatives with NMDA receptor reveals that axial position of phenyl ring is preferable to interact with the binding site, in the other hand the substitution of ortho and para-positions decreases the activity of molecule which was explained in this work by the steric effect, however substitution in meta position enhances the activity, finally the bonding hydrogen formed with nitrogen atom seems to be essential for activity at NMDA receptor.

References

1. Domino E.F., Luby E., Ann Arbor, *NPP Books*, (1981).
2. Huxley A., Fonseca A.S., *Issues Ment. Health Nurs*. 35 (2014) 122.
3. Asenjo L.C., Komossa K., Rummel K.C., Hunger H., Schmid F., Schwarz S., Leucht S., *Cochrane Database Syst. Rev*. CD006633 (2010).
4. Citrome L., *CNS Drugs* 27 (2013) 879.
5. Hartling L., Abou Setta A.M., Dursun S., Mousavi S.S., Pasichnyk D., Newton A.S., *Ann. Intern. Med.* 157 (2012) 498.
6. Leucht S., Corves C., Arbter D., Engel R.R., Li C., Davis J.M., *Lancet* 373 (2009) 31.
7. Naber D., Lambert M., *CNS Drugs* 23 (2009) 649.
8. Lewis D.A., Lieberman J.A., *Neuron* 28 (2000) 325.
9. Angrist B., Sathananthan G., Wilk S., *J. Psychiatr. Res.* 11 (1974) 13.
10. Jentsch J.D., Clin. Neurosci. Res. 3 (2003) 303.
11. Javitt D.C., Zukin S.R., *Am. J. Psychiatry* 148 (1991) 1301.
12. Bakker C.B., Amini F.B., *Compr. Psychiatry* 2 (1961) 269.
13. Jentsch J.D., Roth R.H., *Neuropsychopharmacology* 20 (1999) 201.

14. Mouri A., Noda Y., Nabeshima T., *Int.* 51 (2007) 173.
15. Castellani S., Adams P.M., *Neuropharmacology* 20 (1981) 371.
16. Adams B., Moghaddam B., *J. Neurosci.* 18 (1998) 5545.
17. Bazoui H, Zahouily M., Sebti S., Boulaajaj S., Zakarya D., *J. Mol. Model.* 8 (2002) 1.
18. Bazoui H., Zahouily M., Boulaajaj S., Sebti S., Zakarya D., *Environ Res.* 13 (2002) 567.
19. Kubinyi H., *Wiley Weinheim* 1 (1993).
20. Kubinyi H., *ESCOM Leiden* (1993).
21. Chaudieu I., Vignon J., Chicheportiche M., Kamenka J.M., Trouiller G., Chicheportiche R., *Pharmacol. Biochem. Behav.* 32 (1989) 699.
22. Zhou Z., Parr, R.G., J. *Am. Chem. Soc*. 111 (1989) 7371.
23. Parr R.G., Chattaraj P.K., J. *Am. Chem. Soc*. 113 (1991) 1854.
24. Lee C.T., Yang W.T., Parr R.G., *Phys. Rev*. B 37 (1988) 785.
25. Niecke E., Becker P., Nieger M., Stalke D., Schoeller W.W., Angew. Chem., Int. Ed. Engl. (1995) 34 1849.
26. Frish M.J., Turcks G.W., Schlegel H. B., Scuseria G.E., Robb M.A., Cheeseman J.R., Montgomery J.J. A., Vreven T., Kudin K.N., Burant J.C., Millam J.M., lyengar S.S., Tomasi J., Barone V., Mennucci B., Cossi M., Scalmani G., Rega N., Petersson G.A., Nakatsuji H., Hada M., Ehara M., Toyota K., Fukuda R., Hasegawa J., Ishida M., Nakajima T., Honda Y., Kitao O., Nakai, H., Klene M., Li X., Knox J. E., Hratchian H.P., Cross J.B., Bakken V., Adamo C., Jaramillo J., Gomperts R., Stratmann R.E., Yazyev O., Austin A. J., Cammi R., Pomelli C., Ochterski J.W., Ayala P.Y., Morokuma K., Voth G.A., Salvador P., Dannenberg J.J., Zakrzewski V. G., Dapprich S., Daniels A.D., Strain M.C., Farkas O., Malick D.K., Rabuck A.D., Raghavachari K., Foresman J.B., Ortiz J.V., Cui Q., Baboul A.G., Clifford S., Cioslowski J., Stefanov B.B., Liu G., Liashenko A., Piskorz P., Komaromi I., Martin R.L., Fox D.J., Keith T., Al-Laham M. A., Peng C. Y., Nanayakkara A., Challacombe M., Gill P.M.W., Johnson B., Chen W., Wong M.W., Gonzalez C., Pople J.A. Revision D.01; Gaussian, Inc., Wallingford, CT, (2004).
27. Advanced Chemistry Development Inc., Toronto, Canada (2009).
28. So S.S., Richards G.W., *J. Med. Chem.* 35 (1992) 3201.
29. Andrea T.A., Kalayeh H., *J. Med. Chem.* 34 (1991) 2824.
30. Ellhalaoui M., Thèse de doctorat 106 (2002).
31. Efron B., *J. Am. Stat. Assoc.* 78 (1983) 316.
32. Osten D.W., *J. Chemon*. 2 (1998) 39.
33. Hex, version 8.0.0, ANR-PEPSI (2011-2015)
34. Akyol Z., Gakhar L., Sorensen B. R. Hell J. H., Shea M. A., *Structure* 15 (2007) 1603.
35. The PyMOL Molecular Graphics System, Version 1.8 Schrödinger, LLC.

(2017) ; http://www.jmaterenvironsci.com /